2nd URSI AT-RASC, Gran Canaria, 28 May âĂŞ 1 June 2018

Quasilinear Analysis of Saturation Properties of Broadband Whistler Mode Waves

X. Tao*(1), L. Chen(2), and X. Liu(2)
(1) University of Science and Technology of China, Hefei, China
(2) The University of Texas at Dallas, TX, USA

Abstract

Saturation properties of parallel propagating broadband whistler mode waves are investigated using quasilinear theory. By assuming that the electron distribution stays bi-Maxwellian in the wave excitation process, we combine the previously obtained energy equation of quasilinear theory with linear wave evolution equation to self-consistently model the excitation of broadband whistler mode waves. The resulting evolution profile of wave intensity, spectrum, and electron temperature are consistent with those from particle-in-cell (PIC) simulations. We obtain directly from quasilinear theory that the saturation temperature anisotropy (A) and parallel plasma beta ($\beta_\parallel$) satisfy $A = 0.24/\beta_\parallel^{0.67}$. Our A-$\beta_\parallel$ relation agrees very well with previous results from observation [1] and PIC simulation [2]. We also investigate the dependence of wave saturation amplitude and spectral properties such as bandwidth and peak frequency on various initial and final plasma properties. Our analysis demonstrates that it might be possible to predict the wave amplitude from the initial maximum linear growth rate alone, but not from the initial plasma $\beta_\parallel$. Also we show that the peak frequency and spectrum width are well defined functions of the final $\beta_\parallel$, but not of the initial $\beta_\parallel$ or the initial maximum linear growth rate. Our study indicates that, in case of broadband waves, it might be possible to bypass time-consuming dynamic calculations and obtain wave amplitude directly from the initial plasma properties. These results might be useful in combining microscopic whistler wave excitation process with global modeling of energetic electron dynamics in the inner magnetosphere.

1 Introduction

Saturation properties of whistler mode waves are important to quantify related wave particle interactions. Previous analysis of saturation properties of whistler mode waves have mainly used particle-in-cell (PIC) simulations [2, 3]. The main advantage of PIC simulations is that all nonlinear wave-particle and wave-wave interactions are included. The main disadvantages of PIC simulations are that sometimes it is difficult to identify the main physical process and that simulations typically have high statistical noise. Saturation properties of broadband waves can also be analyzed using quasilinear theory. Yoon and Seough [4] used quasilinear theory and obtained the anisotropy-beta relations for combined mirror and proton cyclotron instabilities for the case of $T_\perp/T_\parallel > 1$, where T is the temperature and subscripts "$\perp$" and "$\parallel$" denote perpendicular and parallel directions with respect to the background magnetic field. In a companion paper, Seough and Yoon [5] reported the quasilinear analysis for parallel proton cyclotron instability for $T_\perp/T_\parallel > 1$ and parallel firehose instabilities for $T_\perp/T_\parallel < 1$. Kim et al. [6] analyzed the electron temperature anisotropy regulation by whistler mode waves using quasilinear theory within the context of solar wind. In this study, we use quasilinear theory to analyze the saturation properties of broadband whistler mode waves.

Two kinds of saturation properties will be investigated. The first one is plasma properties at saturation; i.e., the inverse relation between temperature anisotropy ($A \equiv T_\perp/T_\parallel - 1$) and the parallel plasma beta ($\beta_\parallel \equiv 8\pi n T_\parallel/B^2$). Here n is the number density, and B is the magnetic field strength. Using linear theory analysis and assuming a bi-Maxwellian distribution for electrons, Gary and Wang [3] pointed out that there exists an upper bound on the electron temperature anisotropy due to the excitation of whistler mode waves, and the threshold temperature anisotropy satisfies the relationship

$$\frac{T_\perp}{T_\parallel} - 1 = S/\beta_\parallel^\alpha, \tag{1}$$

where S and α are two fitting constants. This constraint on A was then confirmed by 2D PIC simulations [3]. However, in linear analysis, an assumption about the maximum linear growth rate (γ_m) is needed to obtain values for S and α. The other kind of properties to be investigated are the saturation properties of waves, including saturation amplitude, the peak frequency, and the spectrum width. These parameters are important to estimate effects of waves on particle dynamics.

2 Quasilinear theory

2.1 Review of quasilinear theory

In this paragraph, we briefly review the quasilinear theory for parallel propagating waves and especially the energy equations of Ossakow et al. [7], and describe how we use

the equations to study the evolution and saturation properties of broadband whistler waves. From standard quasilinear theory for parallel propagating waves, Ossakow et al. [7] obtained

$$K_\perp(t) + \sum_k (|B_k|^2/8\pi)\left[2 + (\omega_p^2/k^2c^2)\right] = C_\perp, \quad (2)$$

$$K_\parallel(t) - \sum_k (|B_k|^2/8\pi)\left[1 + (\omega_p^2/k^2c^2)\right] = C_\parallel. \quad (3)$$

Here $K_{\perp,\parallel} = \langle m v_{\perp,\parallel}^2/2\rangle$ are the average perpendicular and parallel kinetic energy of electrons, ω_p is the plasma frequency, c is the speed of light in vacuum, and B_k is the magnetic field amplitude of the $k_{\rm th}$ mode. The two constants $C_\perp$ and $C_\parallel$ depend only on the initial conditions. Equations (2)-(3) essentially describe the transfer of perpendicular kinetic energy to the wave field and the parallel kinetic energy, as whistler waves are driven unstable. As wave energy grows, $K_\perp$ decreases and $K_\parallel$ increases, or A decreases and $\beta_\parallel$ increases. This is the quasilinear relaxation of the electron temperature anisotropy by interactions with whistler mode waves. For other details of the theory, we refer readers to Ossakow et al. [7].

In Equations (2)-(3), the parallel and perpendicular average kinetic energy are related to the corresponding temperature by $T_\perp \equiv m\langle v_\perp^2\rangle/2 = K_\perp$ and $T_\parallel \equiv m\langle v_\parallel^2\rangle = 2K_\parallel$. Within the quasilinear framework, the wave growth is described by linear theory; therefore, the equation describing wave energy evolution of the $k_{\rm th}$ mode is simply

$$\frac{\partial |B_k|^2}{\partial t} = 2\gamma_k |B_k|^2, \quad (4)$$

where γ_k is the linear growth rate of the $k_{\rm th}$ mode. If we assume that the distribution stays as a bi-Maxwellian distribution [3, 4, 5], then γ_k can be calculated directly from the parallel and perpendicular temperature. Taking the time derivative of Equations (2)–(3), we have the needed differential equations to describe the time evolution of the electron temperature,

$$\frac{{\rm d}T_\perp}{{\rm d}t} = -\sum_k 2\gamma_k \frac{|B_k|^2}{8\pi}\left[2 + (\omega_p^2/k^2c^2)\right], \quad (5)$$

$$\frac{{\rm d}T_\parallel}{{\rm d}t} = \sum_k 4\gamma_k \frac{|B_k|^2}{8\pi}\left[1 + (\omega_p^2/k^2c^2)\right]. \quad (6)$$

Similar equations have been derived by Seough and Yoon [5] for EMIC waves.

Equations (4)-(6) are the main equations used in this study to analyze excitation and saturation of whistler mode waves. We choose 100 k's, corresponding to those of whistler mode waves with frequency between 0.05Ω and 0.95Ω, and assume a small initial noise level (e.g., by setting $|B_k|^2 = 10^{-5}$ for all k's). Then by solving the closed set of Equations (4)-(6), we self-consistently track the evolution of whistler waves and the parallel and perpendicular temperature of electrons based on quasilinear theory.

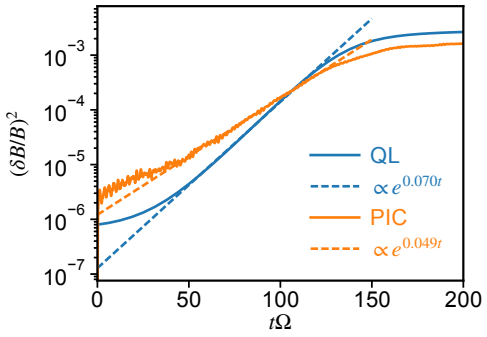

Figure 1. Comparison between quasilinear results (solid orange lines) and PIC simulation results (solid blue lines). Dashed lines denote the power law fitting to the linear growth phase.

2.2 Comparison between quasilinear analysis and PIC simulation

Before we analyze the saturation properties of broadband whistler mode waves, we compare the evolution of wave energy between PIC simulation and quasilinear theory for a case. Here we use a one-dimensional electromagnetic PIC simulation code, where field quantities are assumed to vary along z direction and three components of the velocity are retained. Only parallel propagating whistler mode waves are allowed, consistent with the assumption used in our quasilinear analysis. The electron distribution used in the PIC simulation is a single bi-Maxwellian. For the case in this section, the simulation parameters are taken from Ossakow et al. [7]. We use $T_\perp/T_\parallel = 4, \omega_{pe}/|\Omega_e| = 2$, and $w_\parallel/c = 0.07$, where $w_\parallel$ is the parallel thermal velocity. For this PIC simulation, we use 1024 simulation cells and 2000 number of particles per cell. The cell size is $\Delta z = 0.05c/\Omega$, and the time step is $\Delta t = 0.02\Omega^{-1}$.

Figure 1 shows the evolution of wave intensity from PIC simulation and the quasilinear analysis. The initial noise level of the wave field in quasilinear analysis is chosen to roughly match that of the PIC simulation. We fit the linear growth phase of the wave intensity from PIC simulation and quasilinear analysis by $C_0 \exp^{C_1 t}$, where C_0 and C_1 are two constants. Clearly, $C_1 = 2\bar{\gamma}$, where $\bar{\gamma}$ is the average linear growth rate. From Figure 1, $\bar{\gamma}/\Omega \approx 0.025$ for PIC simulation and 0.035 for quasilinear analysis. The difference of the saturation intensity between quasilinear theory analysis and the PIC simulation is within a factor of two. Considering the approximations made in the quasilinear analysis, we conclude that results from the quasilinear analysis roughly agree with those from PIC simulation, and that quasilinear theory can roughly capture the main physical process in the evolution of broadband whistler mode waves.

3 Saturation properties of broadband whistler mode waves

In the following quasilinear analysis, we use 10 initial $\beta_{\parallel}$'s logarithmically evenly spaced between 10^{-1} and 10. We select 12 initial A's. There are 10 logarithmically evenly spaced A's between 10^0 and 10^1. We add $A = 0.25$ and 0.5 so that some of the initial conditions $(A, \beta_{\parallel})$ fall below the final threshold A-$\beta_{\parallel}$ line, as will be seen below. We also select three ratios of plasma frequency to cyclotron frequency ($\omega_{pe}/\Omega = 2, 4$, and 8) to test the dependence of saturation properties on ω_{pe}/Ω. Some of the selected cases have very large initial linear growth rate, and we have removed all cases with $\gamma_{0m}/\Omega > 1$, where γ_{0m} is the maximum initial linear growth rate. For all cases, we solve Equations (4)-(6) from $t\Omega = 0$ to 600, and verify that the wave field has reached the saturation stage.

3.1 The A–$\beta_{\parallel}$ relationship

Figure 2 shows A and $\beta_{\parallel}$ at $t = 0$ and after wave saturation for all cases calculated. It clearly shows that the final A-$\beta_{\parallel}$ relation from quasilinear theory can be well fit by Equation (1) with $S = 0.24$ and $\alpha = 0.67$, and fitting parameters S and α are independent of ω_{pe}/Ω. To quantify the goodness of regression, we use the R^2 parameter, which is defined by

$$R^2 = 1 - \frac{\sum_i (y_i - f_i)^2}{\sum_i (y_i - \langle y_i \rangle)^2}, \qquad (7)$$

where y_i is the $i_{\rm th}$ value of the dependent variable, f_i is the value of the fitting function for the $i_{\rm th}$ independent variable x_i, and $\langle y_i \rangle$ is the mean value of y_i. For the current case, $y = A, x = \beta_{\parallel}$, and $f = 0.24/\beta_{\parallel}^{0.67}$. The parameter R^2 takes value between 0 and 1. An R^2 of 1 suggests that the regression line perfectly fits the data. For this case, $R^2 = 0.997$ suggests that $A = 0.24/\beta_{\parallel}^{0.67}$ can well describe the relationship between A and $\beta_{\parallel}$ at saturation.

For comparison, we also plot the $A = S/\beta_{\parallel}^{\alpha}$ line with $S = 0.42$ and $\alpha = 0.50$ from Gary and Wang [3], and $S = 0.21$ and $\alpha = 0.60$ from Gary et al. [1]. As can be seen, the quasilinear results agree surprisingly well with those from Gary et al. [1], based on Cluster observations in the magnetosheath. Compared with Gary and Wang [3], our temperature anisotropy upper bound is smaller by about 0.05 for $\beta_{\parallel} \sim 0.1$ and about 0.2 for $\beta_{\parallel} \sim 20$. Note that the temperature anisotropy upper bound from 2D PIC simulation results from An et al. [2] are consistently lower than the one from Gary and Wang [3] by about $0.1 \sim 0.2$ for $10^{-1} \leq \beta_{\parallel} \lesssim 4$; therefore, we conclude that the quasilinear theory results agree very well with PIC simulation results for this $\beta_{\parallel}$ range. Our analysis suggest that the saturation A-$\beta_{\parallel}$ relation can be well described by quasilinear theory for this $\beta_{\parallel}$ range, even though we assumed that the distribution stays bi-Maxwellian.

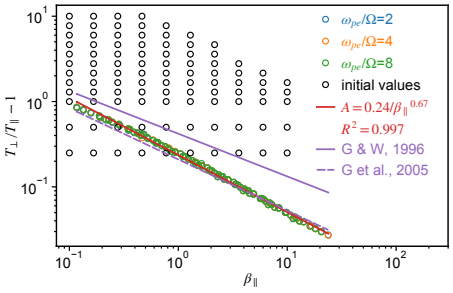

Figure 2. The A-$\beta_{\parallel}$ relation at saturation from quasilinear analysis. The solid red line is the fitting using A=$S/\beta_{\parallel}^{\alpha}$. Black circles denote initial conditions, while color circles denote saturation conditions. The solid purple line denotes the A-$\beta_{\parallel}$ relation from PIC simulation results from Gary and Wang [3]; the dashed purple line, Gary et al. [1].

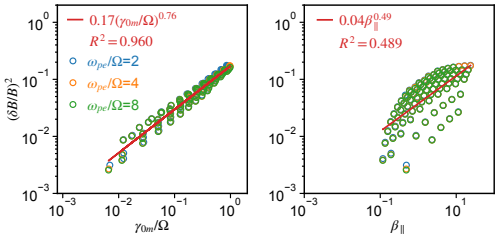

Figure 3. The normalized saturated wave magnetic field energy as a function of the initial γ_{0m} (left) and the $\beta_{\parallel}$ at saturation.

3.2 The dependence of the saturation wave properties on plasma parameters

In this section, we investigate the dependence of the saturation wave amplitude, the peak frequency, and spectrum width at saturation on plasma parameters.

Figure 3 (left) shows the normalized saturation intensity as a function of maximum initial linear growth rate, γ_{0m}. We fit the saturation amplitude using a power law function, and the resulting fitting function is $0.17(\gamma_{0m}/\Omega)^{0.76}$. Note that there is larger spread at smaller γ_{0m}. However, for a given γ_{0m}, the difference between maximum and minimum saturation intensity is within a factor of 2. Figure 3 (right) shows the dependence of saturation wave intensity as a function of $\beta_{\parallel}$ at saturation. We fit the saturation intensity as a function of $\beta_{\parallel}$ using a power law function, following An et al. [2]. The $(\delta B/B)^2$ scales with $\beta_{\parallel}$ roughly as $\beta_{\parallel}^{0.5}$. If we only compare the saturation intensity for $0.1 \leq \beta \leq 3$, we see that the saturation intensity $(\delta B/B)^2$ is consistent with that from [2]. Comparing the left and right panels of Figure 3, we conclude that it might be possible to predict $(\delta B/B)^2$ based on γ_{0m}, but not $\beta_{\parallel}$ at saturation, since $(\delta B/B)^2$ is not a well-defined single-value function of $\beta_{\parallel}$.

Figure 4 shows the normalized peak frequency $\omega_{\rm max}/\Omega$ and

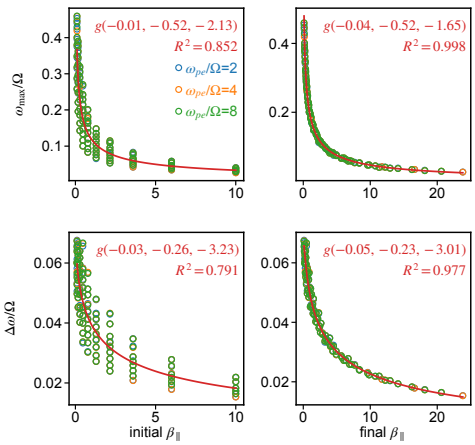

Figure 4. The peak wave frequency (top) and the spectrum width (bottom) as a function of the initial $\beta_\parallel$ (left) and the final $\beta_\parallel$ (right). Red lines are fitting functions using the form given by Equation (8).

the spectrum width $\Delta\omega/\Omega$ as a function of the initial $\beta_\parallel$ and the final $\beta_\parallel$. Denoting the wave power spectral density as $P(\omega)$, the peak frequency is the frequency with maximum intensity; i.e., $P_{\max} = P(\omega_{\max})$. The spectrum width, $\Delta\omega$, is defined as the difference between two frequencies ω_1 and ω_2 which satisfy $P(\omega_1) = P(\omega_2) = P_{\max}/10$. From Figure 4, both $\omega_{\max}$ and $\Delta\omega$ are better correlated with $\beta_\parallel$ at saturation than with initial $\beta_\parallel$. After some experimentation, we choose to fit data using the analytical function of the following form

$$g(a,b,c) = \exp[a(\ln\beta_\parallel)^2 + b\ln\beta_\parallel + c]. \qquad (8)$$

The corresponding parameters are shown in Figure 4 for all four panels. The R^2 parameters are close to 1 for the right two panels of Figure 4, suggesting that the chosen function g can almost perfectly describe the relationship between $\omega_{\max}$ and $\Delta\omega$ as a function of the final $\beta_\parallel$. From left panels of Figure 4, the peak frequency and the frequency width cannot be well predicted from the initial $\beta_\parallel$. We have also experimented with initial γ_{0m} and the initial A, both parameters give even worse results than the initial $\beta_\parallel$.

4 Summary

In this work, we used quasilinear theory to analyze the saturation properties of parallel propagating broadband whistler mode waves in a plasma where electrons have a single bi-Maxwellian distribution. Specifically, we investigated the A-$\beta_\parallel$ relationship and the dependence of saturation amplitudes, peak frequency, and frequency width on initial linear properties and the saturation $\beta_\parallel$. Using self-consistent quasilinear analysis, the obtained A-$\beta_\parallel$ relation agrees very well with observations in the magnetosheath using Cluster measurement [1]. Our A-$\beta_\parallel$ relation also agrees with recent 2D PIC simulations, and the Van Allen Probes observation in the high $\beta_\parallel$ ($\beta_\parallel > 0.1$) regime. Unlike linear theory [3], there is no need to choose an initial maximum linear growth, and the inverse relationship between A and $\beta_\parallel$ is directly given in quasilinear theory. Compared with PIC simulation, the quasilinear theory analysis does not suffer from high statistical noise, and it helps to identify that the main physical process involved in the evolution and saturation of broadband whistler mode waves can be well described by quasilinear theory.

We investigated the relationship between saturation amplitude $(\delta B/B)^2$ and the maximum initial linear growth rate γ_{0m} and $\beta_\parallel$ at saturation. We showed that it is possible to predict $(\delta B/B)^2$ from initial γ_{0m}. This conclusion might be useful when predicting whistler mode wave amplitude from global non-self-consistent wave modeling codes. We demonstrated that the peak frequency and the spectrum width are well defined functions of $\beta_\parallel$ at saturation, but not of the initial $\beta_\parallel$. We showed that both $\omega_{\max}$ and $\Delta\omega$ might be modeled as a function of $\beta_\parallel$ at saturation using analytical form $g(a,b,c) = \exp[a(\ln\beta_\parallel)^2 + b\ln\beta_\parallel + c]$, where a, b, and c are three parameters. The R^2 parameters for both fittings are close to 1.

References

[1] S. P. Gary, B. Lavraud, M. F. Thomsen, B. Lefebvre, and S. J. Schwartz, "Electron anisotropy constraint in the magnetosheath: Cluster observations," *Geophys. Res. Lett.*, **32**, 13, 2005, L13109.

[2] X. An, C. Yue, J. Bortnik, V. Decyk, W. Li, and R. M. Thorne, "On the parameter dependence of the whistler anisotropy instability," *Journal of Geophysical Research: Space Physics*, **122**, 2, 2017, pp. 2001–2009.

[3] S. P. Gary and J. Wang, "Whistler instability: Electron anisotropy upper bound," *J. Geophys. Res.*, **101**, A5, 1996, pp. 10,749–10,754.

[4] P. H. Yoon and J. Seough, "Quasilinear theory of anisotropy-beta relation for combined mirror and proton cyclotron instabilities," *J. Geophys. Res.*, **117**, 2012, A08102.

[5] J. Seough and P. H. Yoon, "Quasilinear theory of anisotropy-beta relations for proton cyclotron and parallel firehose instabilities," *J. Geophys. Res.*, **117**, 2012, A08101.

[6] H. P. Kim, J. Hwang, J. J. Seough, and P. H. Yoon, "Electron temperature anisotropy regulation by whistler instability," *J. Geophys. Res. Space Physics*, **122**, 4, 2017, pp. 4410–4419.

[7] S. L. Ossakow, E. Ott, and I. Haber, "Nonlinear evolution of whistler instabilities," *Phys. Fluids*, **15**, 12, 1972, pp. 2314–2326.